Available online at www.sciencedirect.com
SCIENCE DIRECT
International Journal of Mass Spectrometry 254 (2006) 145–151
International Journal of Mass Spectrometry
www.elsevier.com/locate/ijms

Dehydrogenation of formic acid catalyzed by magnesium hydride anions, $HMgL_2^-$ (L = Cl and HCO_2)

George N. Khairallah [a,b], Richard A.J. O'Hair [a,b,*]

[a] School of Chemistry, The University of Melbourne, Vic. 3010, Australia
[b] Bio21 Institute of Molecular Science and Biotechnology, The University of Melbourne, Vic. 3010, Australia

Received 31 January 2006; received in revised form 20 April 2006; accepted 24 April 2006
Available online 5 June 2006

Abstract

A two step gas-phase catalytic cycle for the dehydrogenation of formic acid was established using a combination of experiments carried out on a quadrupole ion trap mass spectrometer and DFT calculations. The catalysts are the magnesium hydride anions $HMgL_2^-$ (L = Cl and HCO_2), which are formed from the formate complexes, $HCO_2MgL_2^-$, via elimination of carbon dioxide under conditions of collision induced dissociation. This is followed by an ion–molecule reaction between $HMgL_2^-$ and formic acid, which yields hydrogen and also reforms the formate complex, $HCO_2MgL_2^-$. A kinetic isotope effect in the range 2.3–2.9 was estimated for the rate determining decarboxylation step by carrying out CID on the $(HCO_2)(DCO_2)MgCl_2^-$ and subjecting the resultant mixture of $(H)(DCO_2)MgCl_2^-$ and $(HCO_2)(D)MgCl_2^-$ ions at *m/z* 106 to ion–molecule reactions. DFT calculations (at the B3LYP/6−31 + G* level of theory) were carried out on the $HMgCl_2^-$ system and revealed that: (i) the decarboxylation of $HCO_2MgCl_2^-$ is endothermic by 47.8 kcal mol^{-1}, consistent with the need to carry out CID to form the $HMgCl_2^-$; (ii) $HMgCl_2^-$ can react with formic acid via either a four centred transition state or a six centred transition state. The former reaction is favoured by 7.8 kcal mol^{-1}.

Keywords: Catalysis by metal hydrides; Magnesium formate anions; Electrospray ionisation; Multistage mass spectrometry; Collision induced dissociation; Decarboxylation; Ion–molecule reactions; Density-functional calculations

1. Introduction

The reactions which inter-convert the three sets of reactants/products: formic acid/water and carbon monoxide/hydrogen and carbon dioxide (Fig. 1) continue to attract considerable attention, especially within the context of designing metal catalysts to direct a specific reaction channel. Reactions (1) and (2) represent the two main decomposition channels of formic acid and have been widely studied experimentally [1] and theoretically [2]. In the gas phase, in the absence of catalysts, the dehydration channel (Reaction (1), Fig. 1) is the dominant reaction [1], consistent with a lower activation energy, as predicted by DFT calculations [2]. A number of studies have demonstrated that metal catalysts can favour the decarboxylation of formic acid (Reaction (2), Fig. 1) [3], an undesirable process within the context of formic acid treatment of nuclear wastes [4]. The reverse reaction, hydrogenation of CO_2, is of topical interest as a means converting a greenhouse gas to an industrially useful chemical [5]. Once again, metal catalysts play an important role in these reactions, and DFT calculations on model systems reveal a substantial drop in the barriers relative to the uncatalyzed reaction [6]. Reaction (3) is the widely studied"water gas shift" process [7], which provides a way of producing hydrogen gas via the use of transition metal catalysts [4,6a]. Given the importance of the reactions shown in Fig. 1, it is surprising that few studies have used mass spectrometry based experiments to examine the role of metal ions in mediating related processes in the gas phase. Of relevance are early studies on the reactions of bare atomic metal ions with formic acid [8] and Squires' studies on the gas phase chemistry of $(CO)_4FeCO_2H^-$, a proposed intermediate of the water gas shift process [9]. During the course of our work, a paper has appeared on the decarboxylation of $[Pd(PPh_3)_2(OCOH)]^+$ as probed via ESI/FT-ICR MS [10].

Electrospray ionisation (ESI) coupled with quadrupole ion trap mass spectrometry (QIT-MS) has proven to be a powerful way of examining metal mediated processes, including gaining

* Corresponding author. Tel.: +61 3 8344 2452; fax: +61 3 8347 5180.
E-mail address: rohair@unimelb.edu.au (R.A.J. O'Hair).

1387-3806/$ – see front matter © 2006 Elsevier B.V. All rights reserved.
doi:10.1016/j.ijms.2006.04.011

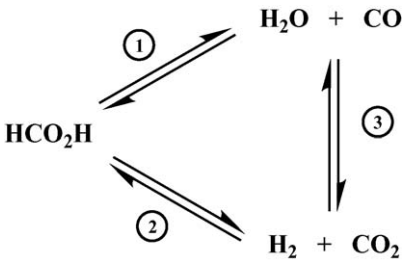

Fig. 1. Different reactions which process the sets of reactants/products: formic acid/water and carbon monoxide/hydrogen and carbon dioxide. Reactions 1 and 2 relate to the decomposition of formic acid. Reaction 3 is the "water gas shift" process.

detailed insights into catalytic cycles [11]. To date, we have discovered catalytic cycles for the oxidation of methanol to formaldehyde [12], and the decomposition of acetic acid via two different pathways (Fig. 2) [13]. The latter studies are of particular relevance within the context of Fig. 1, since they highlight the importance of the nature of the metal catalyst in enhancing the selective decomposition of a related carboxylic acid, acetic acid via either dehydration (Reaction (4)) or decarboxylation (Reaction (5)). We have found that group VI mononuclear $[MO_3(OH)]^-$ and binuclear $[M_2O_6(OH)]^-$ oxo-anions (where M = Mo and W) selectively catalyze the ketene pathway (Reaction (4) and Fig. 2a) [13a], while the organomagnesate $[CH_3MgL_2]^-$ (L = Cl and = O_2CCH_3), favour the decarboxylation pathway (Reaction (5) and Fig. 2b) [13b]. Here, we use a combination of quadrupole ion trap mass spectrometry experiments and DFT calculations to examine whether the decarboxylation of formic acid can be catalyzed by the related magnesium hydride anions $[HMgL_2]^-$ (L = Cl and O_2CH) [14].

$$CH_3CO_2H \rightarrow CH_2CO + H_2O \quad (4)$$

$$CH_3CO_2H \rightarrow CO_2 + CH_4 \quad (5)$$

2. Experimental

2.1. Reagents

Formic acid (HPLC grade, 99.5%) and deuterated formic-D-acid-D (95%, 98% D incorporation) were obtained from Aldrich and used without further purification.

2.2. Mass spectrometry

Mass spectrometry experiments were conducted using a modified Finnigan LCQ quadrupole ion trap mass spectrometer equipped with a Finnigan electrospray ionisation source, as described previously [13]. Magnesium formate anions $[(HCO_2)_{3-x}MgCl_x]^-$, were prepared by electrospraying a mixture of $MgCl_2$ and formic acid in methanol (0.2 mM). Related magnesium $[(RCO_2)_{3-x}MgCl_x]^-$ anions have been reported upon electrospraying mixtures of $MgCl_2$ and other carboxylic acids [13b,15]. The ESI solution was pumped into the electrospray source at approximately 3 μL/min. Typical electrospray source conditions involved needle potentials of 4.0–4.5 kV and heated capillary temperatures of 170–200 °C. Extensive tuning of the electrospray conditions was often required due to the low signal-to-noise ratio and/or low abundance of some species. Mass selection and collisional activation were carried out using standard isolation and excitation procedures using the 'advanced scan' function of the LCQ software.

The instrument has been modified to permit introduction of neutral reagents into the ion trap, allowing the measurement of ion–molecule reactions, and these modifications and experimental procedures have been described in detail previously [13]. Gronert's pioneering studies suggest that ions undergoing ion–molecule reactions in the LCQ are essentially at room temperature [16]. Unfortunately, the magnesium hydride anions are highly reactive, which precludes measurement of ion–molecule rate constants, consistent with our previous studies on highly reactive organometallics [17].

2.3. DFT calculations

In order to gain qualitative insights into the mechanisms of the formation and reactions of the magnesium hydride anions, we have carried out DFT calculations using Gaussian 03 [18] at the B3LYP level of theory with a 6−31+G* basis set. While an extensive evaluation of the performance of various levels of theory for predicting the structures and energetics of reactions of magnesium hydride anions is lacking [19] to maintain consistency with our previous study [13b], we have used the B3LYP/6−31 + G* level of theory. Optimizations were carried out without any symmetry constraints. Vibrational frequency calculations were carried out on each optimized structure at the same level of theory. Reaction energetics were calculated by using the energies listed in the supplementary material section, with the ZPVE corrected by 0.9806 [20].

2.4. DFT estimated kinetic isotope effect for decarboxylation

The kinetic isotope effect (KIE) for the decarboxylation of $HCO_2MgCl_2^-$ was estimated from statistical mechanics using

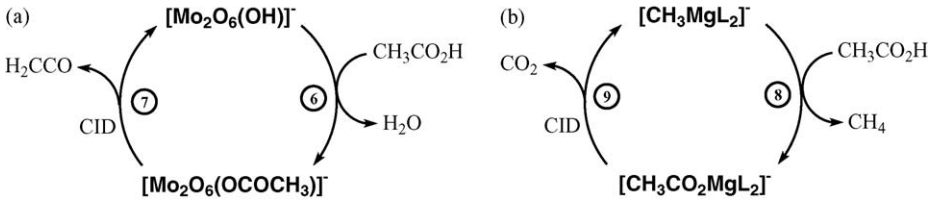

Fig. 2. Gas phase catalytic cycles for the metal mediated: (a) dehydration of acetic acid [13a]; (b) decarboxylation of acetic acid [13b].

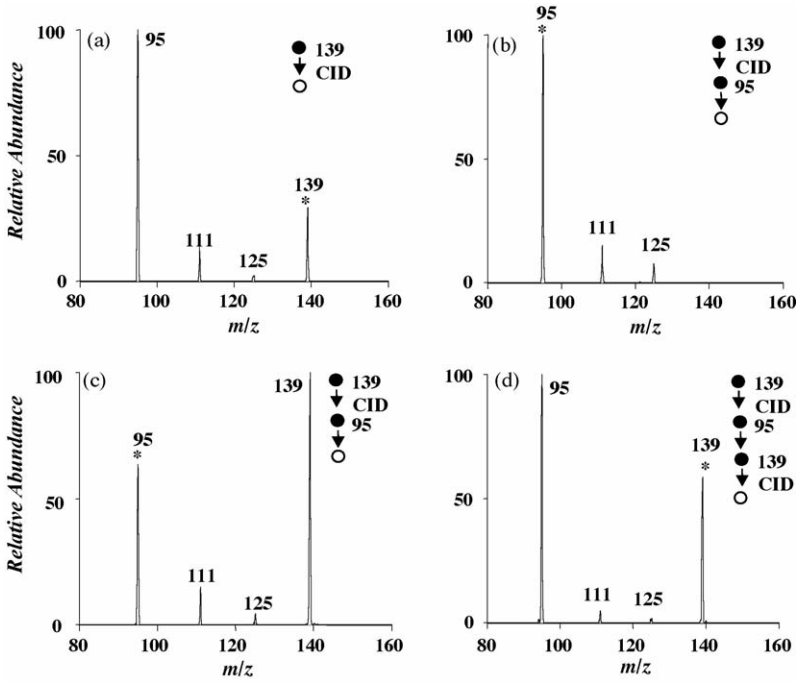

Fig. 3. Multistage (MS^n) QIT-MS experiments on the key two steps for decomposition of HCO_2H catalyzed by $HMgCl_2^-$: (a) MS^2 CID of $HCO_2MgCl_2^-$; (b) MS^3 ion–molecule reactions of mass selected $HMgCl_2^-$ with background water and methanol; (c) MS^3 ion–molecule reactions of mass selected $HMgCl_2^-$ with HCO_2H (introduced into the QIT with a background pressure of ca 2.6×10^{-7} torr); (d) MS^3 CID of $HCO_2MgCl_2^-$ (formed in spectrum 3c).

the procedure described by Zeller and Strassner [21]. Thus, the free activation energies for decarboxylation, ΔG_X, were determined for both the deuterated (X = D) and non-deuterated (X = H) isotopomers of $HCO_2MgCl_2^-$, using Eq. (10), which requires the free energies of both the transition state ($G_X^{\ddagger}$) as well as the reactant (G_X). The KIE is then estimated using Eq. (11). The DFT calculated free energies are listed in the supplementary material (Table S3).

$$\Delta G_X = G_X^{\ddagger} - G_X \text{ (where X = H or D)} \quad (10)$$

$$\text{KIE} = \frac{k_H}{k_D} = e^{(\Delta G_D - \Delta G_H)/RT} \quad (11)$$

3. Results & discussion

3.1. QIT mass spectrometry experiments on the decarboxylation of formic acid catalysed by $HMgL_2^-$ (L = Cl and HCO_2)

Negative ion electrospray mass spectrometry of a mixture of magnesium chloride and formic acid yields a range of anions including $HCO_2MgCl_2^-$, $(HCO_2)_2MgCl^-$ and $(HCO_2)_3Mg^-$. Although each of these anions appear to be unreactive towards formic acid, a hidden identity exchange metathesis reaction (Reaction (12)) is revealed upon using deuterium labelled formic acid (as illustrated in supplementary Fig. S1 for the $HCO_2MgCl_2^-$ ion).

$$HCO_2MgL_2^- + DCO_2D \rightarrow DCO_2MgL_2^- + HCO_2D \quad (12)$$

The magnesium formate anions all undergo decarboxylation under collision induced dissociation conditions (Reaction (13) to yield the magnesium hydride anions, as illustrated in Fig. 3a for the $HCO_2MgCl_2^-$ ion. The competing loss of formate anion (Reaction (14)) does not appear to operate, although the detection of this low mass ion (*m/z* 45) is challenging in the ion trap. The highly reactive magnesium hydride anions readily react with background water and methanol (from the ESI solvent) via acid base reactions (Reaction (15), A = HO and CH_3O), as shown for the mass selected $HMgCl_2^-$ ion in Fig. 3b. When formic acid is introduced into the mass spectrometer, the mass selected magnesium hydride anions react to regenerate the magnesium formate anions (Reaction (15), A = HCO_2), as illustrated for the $HMgCl_2^-$ ion in Fig. 3c, which undergo the same decarboxylation step in a MS^4 experiment (Fig. 3d). This completes a formal catalytic cycle for the dehydrogentation of formic acid, as shown in Fig. 4. In fact, we have been able to demonstrate that this is a genuine catalytic cycle by using the same population of $HMgL_2^-$ catalysts to traverse the catalytic cycle a total of three times (a MS^7 experiment). We have not gone beyond the MS^7 experiment, nor have we the tried to quantify the overall efficiency of the catalytic cycle. It is worth noting, however, that there is loss of signal during each step of the catalytic cycle.

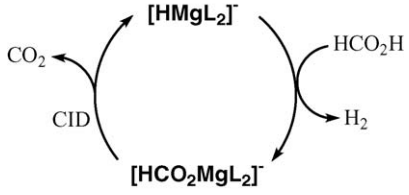

Fig. 4. Gas phase catalytic cycle for the dehydrogenation of formic acid mediated by the magnesium hydride anions, $HMgL_2^-$.

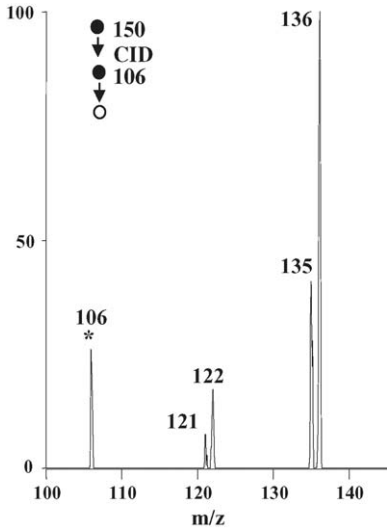

Fig. 5. Determination of the kinetic isotope effect for decarboxylation of the $[(HCO_2)(DCO_2)MgCl]^-$ ion via ion–molecule reactions of the $[(HCO_2)(DCO_2)MgCl–CO_2]^-$ ion with background water and methanol. See Scheme 1 and text for discussion of isotope effect.

Thus, some signal loss occurs during the CID step, and this may arise from ejection of the precursor ion from the trap or from competing formate anion loss (Reaction (14)). Similarly, some loss of signal occurs during the ion–molecule reaction of the $HMgL_2^-$ with formic acid (Reaction (15), A = HCO_2), and this arises from competing reactions with background water and methanol (Reaction (15), A = HO and CH_3O), as shown in Fig. 3c.

$$HCO_2MgL_2^- \rightarrow HMgL_2^- + CO_2 \quad (13)$$

$$HCO_2MgL_2^- \rightarrow HCO_2^- + MgL_2 \quad (14)$$

$$HMgL_2^- + AH \rightarrow AMgL_2^- + H_2 \quad (15)$$
$$(A{=}HO, CH_3O \text{ and } HCO_2)$$

Since the decarboxylation reaction (Reaction (13)) is clearly the rate determining step, we utilized the acid–base reactions to estimate the kinetic isotope effect (KIE) for the decarboxylation of the $(HCO_2)(DCO_2)MgCl^-$ ion (Fig. 5 and Scheme 1). Thus, decarboxylation of this ion yields both the magnesium hydride $(H)(DCO_2)MgCl^-$ (path a of Scheme 1) and magnesium deuteride $(HCO_2)(D)MgCl^-$ anions (path b of Scheme 1). As both of these product ions have the same mass, they cannot be distinguished in the MS/MS experiments. However, when this $[(HCO_2)(DCO_2)MgCl–CO_2]^-$ product ion is mass selected and allowed to react with background water and methanol, the isotope effect is revealed as the products from the acid–base ion–molecule reactions, $ROMg(Cl)(O_2CD)^-$ (path a of Scheme 1) and $ROMg(Cl)(O_2CH)^-$ (path b of Scheme 1) now have a different mass. While it is likely that there is an isotope effect for the acid–base reactions, by allowing the $[(HCO_2)(DCO_2)MgCl–CO_2]^-$ ion to react for 300 ms, greater than 85% conversion to $ROMg(Cl)(O_2CD)^-$ and $ROMg(Cl)(O_2CH)^-$ ions is achieved. Using these product ion abundances, the following estimates of the KIE for decarboxylation can be made: $k_H/k_D = 2.9$ (comparing abundances of $HOMg(Cl)(O_2CD)^-$ (*m/z* 122) and $HOMg(Cl)(O_2CH)^-$ (*m/z* 121)) and $k_H/k_D = 2.3$ (comparing abundances of $CH_3OMg(Cl)(O_2CD)^-$ (*m/z* 136) and $CH_3OMg(Cl)(O_2CH)^-$ (*m/z* 135)). Thus, the KIE is quite large, consistent with the cleavage of a C–H bond in the rate determining step. Interestingly, this estimated KIE (in the range 2.3–2.9) is larger than that for elimination of: acetaldehyde from $[Mo_2O_6(OCH_2CH_3)]^-$ ($k_H/k_D = 1.9 \pm 0.4$) [12b] and methylketene from $[Mo_2O_6(O_2CCH_2CH_3)]^-$ (k_H/k_D in the range 1.3–1.5) $[W_2O_6(O_2CCH_2CH_3)]^-$ (k_H/k_D in the range 1.4–1.6) and $[MoO_3(O_2CCH_2CH_3)]^-$ (k_H/k_D in the range 1.5–1.8) [13a].

3.2. DFT calculations on the decarboxylation of formic acid catalysed by $HMgCl_2^-$

In order to gain further evidence that the magnesium hydride anions catalyze the decarboxylation of formic acid, we have used DFT calculations (at the B3LYP/6−31 + G* level of theory to gain insights into the structures and energetics of the key species on the potential energy surfaces of the decarboxylation reaction (Fig. 3a, Reaction (13)) and the acid–base reaction (Reaction (15)) for the $HMgCl_2^-$ system. The energy profile for two competing pathways of decarboxylation (Reaction (13)) and formate loss (Reaction (14)) are shown in Fig. 6, while the structures for all species are given in the supplementary material (Fig. S2). An examination of Fig. 6 clearly reveals that the

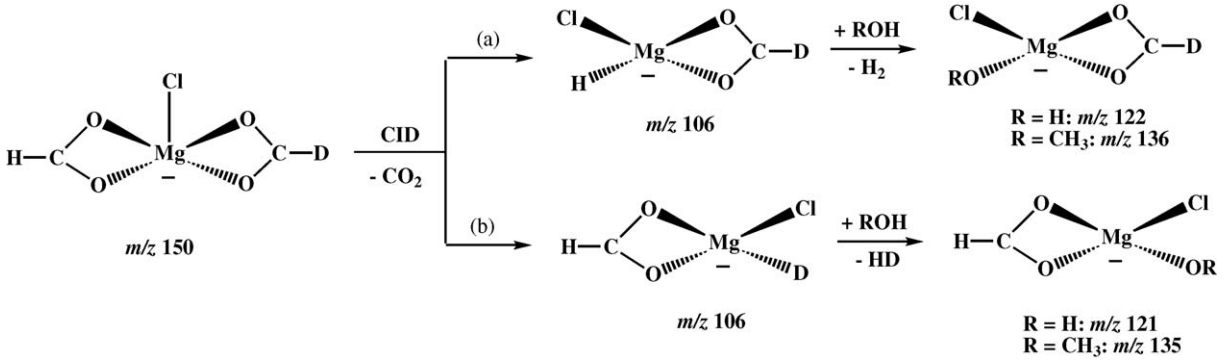

Scheme 1. Determination of the kinetic isotope effect for decarboxylation of the $[(HCO_2)(DCO_2)MgCl]^-$ based on the products from ion–molecule reactions of the $[(HCO_2)(DCO_2)MgCl–CO_2]^-$ ion with background water and methanol.

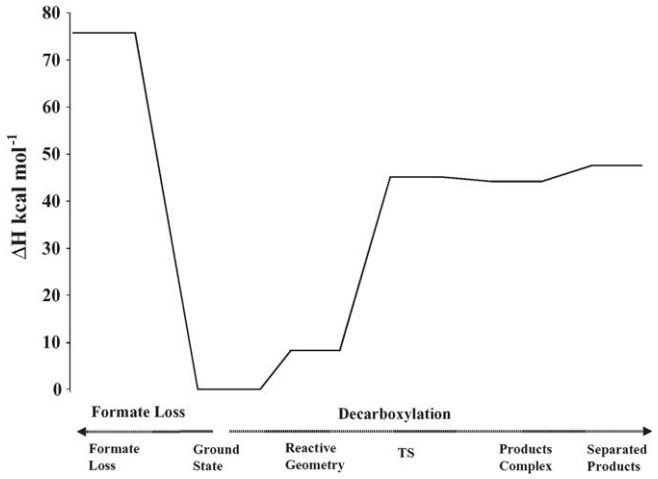

Fig. 6. Plot of B3LYP/6−31 + G* calculated reaction coordinate for CO_2 loss (right hand side) from $[HCO_2MgCl_2]^-$ (Reaction (13)) versus the energetics for formate loss (Reaction (14), left hand side).

decarboxylation reaction is favoured over the formate loss channel. The DFT calculated vibrational frequencies can be used to estimate the kinetic isotope effect (KIE) for the decarboxylation of $HCO_2MgCl_2^-$. Using the approach described in Section 2, a KIE of $k_H/k_D = 4.9$ was estimated using the ground state structure of the $HCO_2MgCl_2^-$(here the formate binds in a bidentate fashion as shown in structure **1** of supplementary Fig. S2). A smaller KIE ($k_H/k_D = 4.6$) is calculated if the reactive geometry is used (here the formate binds in a monodentate fashion as shown in structure **2** of supplementary Fig. S2). These DFT estimates for the decarboxylation are somewhat higher that the experimental estimated range k_H/k_D 2.3–2.9 for decarboxylation of the related $(HCO_2)(DCO_2)MgCl^-$ ion. A possible explanation for this discrepancy is that a modest level of theory is used for the DFT calculations.

Our previous DFT studies on the reactions of the organomagnesium anions, $CH_3MgL_2^-$ (L = Cl and CH_3CO_2) revealed that they reacted with acids to form an initial adduct, which then underwent intramolecular proton transfer with expulsion of methane via either a four or six centred transition state depending on the structure of the initial acid [13b]. Given that formic acid can coordinate to magnesium via its C=O oxygen or its OH oxygen, we have considered both a six centred and a four centred transition state for the acid-base reaction Eq. (15). Fig. 7 compares the energy profiles for both the four centred and the six centred transition states for the reactions of $HMgCl_2^-$ with formic acid, while Fig. 8 shows the structures of key species on the potential energy surfaces of these reactions. An examination of Fig. 7 reveals that both reactions (proceeding via the four centred and the six centred transition states) are viable and have similar overall exothermicities, although that proceeding via the four centred has a lower barrier.

The structures shown in Fig. 8 also reveal some interesting differences between the pathways associated with the four centred and the six centred transition states. Thus, the two different transition states for reaction with formic acid are initiated from two different reactant ion–molecule complexes. The six centred reactant ion–molecule complex involves coordination of the formic acid via the C=O oxygen to the magnesium centre (Fig. 8d). In contrast, the four centred reactant ion–molecule complex involves the formation of a hydrogen bond between the magnesium hydride and the OH of formic acid (Fig. 8c). Related hydrogen bonds involving metal hydrides have been described [22]. The product ion–molecule complexes are also quite different. Thus, that involving the four centred transition state yields a magnesium formate complex in which the formate

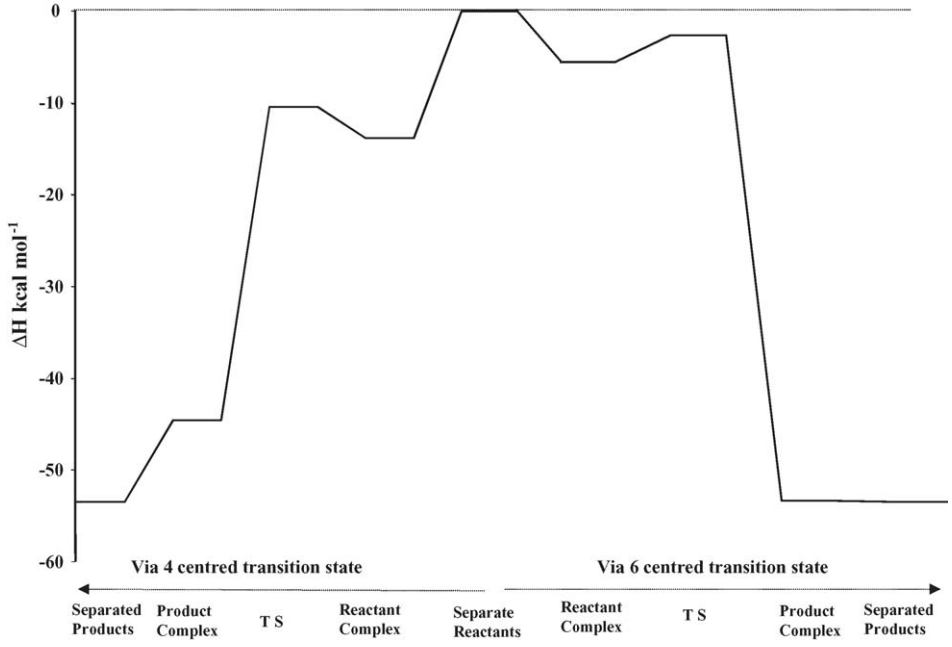

Fig. 7. Plot of B3LYP/6−31 + G* calculated reaction coordinate for ion–molecule reactions of formic acid with $[HMgCl_2]^-$ via (a) four centred transition state (left hand side); (b) six centred transition state (right hand side).

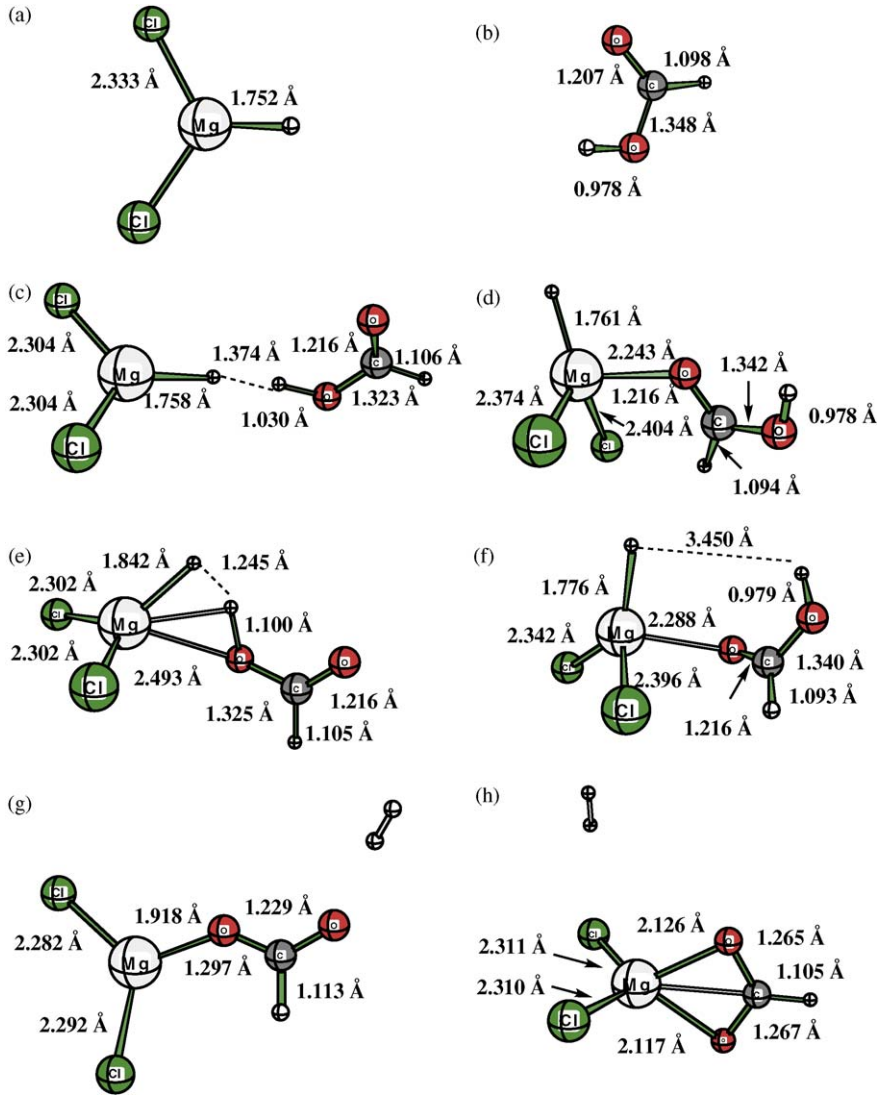

Fig. 8. B3LYP/6−31 + G* optimized structures of key species from the energy surfaces shown in Fig. 8: (a) $HMgCl_2^-$; (b) HCO_2H; (c) reactant ion–molecule complex for four centred transition state; (d) reactant ion–molecule complex for six centred transition state; (e) TS for four centred transition state; (f) TS for six centred transition state; (g) product ion–molecule complex for 4 centred transition state; (h) product ion–molecule complex for six centred transition state. Bond lengths in Å.

ligand is bound in a monodentate fashion (Fig. 8g). In contrast, the product ion–molecule complex derived from the six centred transition state yields a magnesium formate complex in which the formate ligand is bound in a bidentate fashion (Fig. 8h).

4. Conclusions

A two step gas-phase catalytic cycle is presented for the dehydrogenation of formic acid using a combination of experiments carried out on a quadrupole ion trap mass spectrometer and DFT calculations. The catalysts are the magnesium hydride anions $HMgL_2^-$ (L = Cl and HCO_2), which are formed from the formate complexes, $HCO_2MgL_2^-$, via elimination of carbon dioxide under conditions of collision induced dissociation. This is followed by ion–molecule reactions between $HMgL_2^-$ and formic acid, which yields hydrogen and also reforms the magnesium formate complex, $HCO_2MgL_2^-$. A kinetic isotope effect in the range 2.3–2.9 was estimated for the rate determining decarboxylation step, by carrying out CID on the $(HCO_2)(DCO_2)MgCl_2^-$ with ion–molecule reactions. DFT calculations (at the B3LYP/6−31 + G* level of theory) were carried out on the $HMgCl_2^-$ system and revealed that: (i) the decarboxylation of $HCO_2MgCl_2^-$ is endothermic by 47.8 kcal mol^{-1}, consistent with the need to carry out CID to form the $HMgCl_2^-$; (ii) $HMgCl_2^-$ can react with formic acid via either a four centred transition state or a six centred transition state. The former reaction is favoured by 7.8 kcal mol^{-1}. The combination of QIT-MS and DFT calculations is a powerful way of examining gas phase catalysis by ionic metal catalysts.

Acknowledgements

RAJO thanks the Australian Research Council for financial support (Grant #DP0558430). Support of the Victorian Institute

for Chemical Sciences High Performance Computing Facility is gratefully acknowledged.

Appendix A. Supplementary data

Supplementary data associated with this article can be found, in the online version, at doi:10.1016/j.ijms.2006.04.011.

References

[1] K. Saito, T. Shiose, O. Takahashi, Y. Hidaka, F. Aiba, K. Tabayashi, J. Phys. Chem. A 109 (2005) 5352 (and references cited therein).
[2] B. Wang, H. Hou, Y. Gu, J. Phys. Chem. A 104 (2000) 10526 (and references cited therein).
[3] (a) C. Bianchini, M. Peruzzini, A. Polo, A. Vacca, F. Zanobini, Gazz. Chim. Ital. 121 (1991) 543;
(b) J.H. Shin, D.G. Churchill, G. Parkin, J. Organomet. Chem. 642 (2002) 9.
[4] R.B. King, J. Organomet. Chem. 586 (1999) 2.
[5] (a) P.G. Jessop, F. Joo, C.C. Tai, Coord. Chem. Rev. 248 (2004) 2425;
(b) E. Dinjus, R. Fornika, S. Pitter, T. Zevaco, in: B. Cornils, W.A. Herrmann (Eds.), Applied Homogeneous Catalysis with Organometallic Compounds, 3, second ed., Wiley–VCH, Weinheim, 2002, p. 1189.
[6] (a) M. Torrent, M. Sola, G. Frenking, Chem. Rev. 100 (2000) 439;
(b) D.-Y. Hwang, A.M. Mebel, J. Phys. Chem. A 108 (2004) 10245;
(c) D.-Y. Hwang, A.M. Mebel, Chem. Phys. Lett. 396 (2004) 75.
[7] (a) Q. Fu, H. Saltsburg, M. Flytzani-Stephanopoulos, Science 301 (2003) 935;
(b) W.A. Herrmann, M. Muehlhofer, in: B. Cornils, W.A. Herrmann (Eds.), Applied Homogeneous Catalysis with Organometallic Compounds, vol. 3, second ed., Wiley–VCH, Weinheim, 2002, p. 1086.
[8] (a) M. Lombarski, J. Allison, Int. J. Mass Spectrom. Ion Proc. 65 (1985) 31;
(b) R.C. Burnier, G.D. Byrd, B.S. Freiser, Anal. Chem. 52 (1980) 1641.
[9] L.S. Sunderlin, R.R. Squires, J. Am. Chem. Soc. 115 (1993) 337.
[10] R. Qian, H. Guo, Y. Liao, H. Wang, X. Zhang, Y. Guo, Rapid Commun. Mass Spectrom. 20 (2006) 589.
[11] R.A.J. O'Hair, Chem. Comm. (2006) 1469.
[12] (a) T. Waters, R.A.J. O'Hair, A.G. Wedd, Chem. Commun. (2000) 225;
(b) T. Waters, R.A.J. O'Hair, A.G. Wedd, J. Am. Chem. Soc. 125 (2003) 3384;
(c) T. Waters, R.A.J. O'Hair, A.G. Wedd, Inorg. Chem. 44 (2005) 3356.
[13] (a) T. Waters, R.A.J. O'Hair, A.G. Wedd, Int. J. Mass Spectrom. 228 (2003) 599;
(b) R.A.J. O'Hair, A.K. Vrkic, P.F. James, J. Am. Chem. Soc. 126 (2004) 12173.
[14] For a review on the gas phase chemistry of metal hydrides, see:. P.B. Armentrout, L.S. Sunderlin, in: A. Dedieu (Ed.), Transition Metal Hydrides, VCH, 1992, pp. 1–64.
[15] S. Ouyang, M.A. Vairavamurthy, Anal. Chim. Acta 422 (2000) 101.
[16] (a) S. Gronert, J. Am. Soc. Mass Spectrom. 9 (1998) 845;
(b) S. Gronert, J. Am. Chem. Soc. 123 (2001) 3081.
[17] A. Jacob, P.F. James, R.A.J. O'Hair, Do alkali and alkaline earth acetates form organometallates via decarboxylation? A survey using electrospray ionization tadem mass spectrometry and DFT calculations, Int. J. Mass Spectrom. (invited contribution to Professor Bohme Honor Issue), in press (doi:10.1016/j.ijms.2005.08.015).
[18] M.J. Frisch, G.W. Trucks, H.B. Schlegel, G.E. Scuseria, M.A. Robb, J.R. Cheeseman, J.A. Montgomery Jr., T. Vreven, K.N. Kudin, J.C. Burant, J.M. Millam, S.S. Iyengar, J. Tomasi, V. Barone, B. Mennucci, M. Cossi, G. Scalmani, N. Rega, G.A. Petersson, H. Nakatsuji, M. Hada, M. Ehara, K. Toyota, R. Fukuda, J. Knox, H.P. Hratchian, J.B. Cross, C. Adamo, J. Jaramillo, R. Gomperts, R.E. Stratmann, O. Yazyev, A.J. Austin, R. Cammi, C. Pomell, J.W. Ochterski, P.Y. Ayala, K. Morokuma, G.A. Voth, P. Salvador, J.J. Dannenberg, V.G. Zakrzewski, S. Dapprich, A.D. Daniels, M.C. Strain, O. Farkas, D.K. Malick, A.D. Rabuck, K. Raghavachari, J.B. Foresman, J.V. Ortiz, Q. Cui, A.G. Baboul, S. Clifford, J. Cioslowski, B.B. Stefanov, G. Liu, A. Liashenko, P. Piskorz, I. Komaromi, R.L. Martin, D.J. Fox, T. Keith, M.A. Al-Laham, C.Y. Peng, A. Nanayakkara, M. Challacombe, P.M.W. Gill, B. Johnson, W. Chen, M.W. Wong, C. Gonzalez, J.A. Pople, Gaussian_03, Gaussian, Inc., Pittsburgh, PA, 2003.
[19] (a) Note that work on small inorganic magnesium systems suggests that large basis sets are required to get accurate thermochemistry. See:. S. Petrie, L. Radom, Int. J. Mass Spectrom. 192 (1999) 173;
(b) M. Alcami, A.I. Gonzalez, O. Mo, M. Yanez, Chem. Phys. Lett. 307 (1999) 244;
(c) S. Petrie, J. Phys. Chem. A 106 (2002) 5188;
(d) S. Petrie, J. Phys. Chem. A 106 (2002) 7034.
[20] A.P. Scott, L. Radom, J. Phys. Chem. 100 (1996) 16502.
[21] A. Zeller, Th. Strassner, Organometallics 21 (2002) 4950.
[22] N.V. Belkova, E.S. Shubina, L.M. Epstein, Acc. Chem. Res. 38 (2005) 624.